

The electronic structure, optical properties, and phonon transport of a VBi monolayer in the rock-salt phase using the first-principles method

Mustafa M. Jaafar, Jabbar M. Khalaf Al-zyadi* 

Department of Physics, College of Education for Pure Sciences, University of Basrah, Basrah, Iraq

ARTICLE INFO

Received 15 September 2023
Accepted 31 October 2023
Published 30 December 2023

Keywords :

monolayer properties, VBi, half-metallic

Citation: M.M. Jaafar, J. M. Khalaf Al-zyadi, J. Basrah Res. (Sci.) 49(2), 197 (2023).
[DOI:https://doi.org/10.56714/bjrs.49.2.16](https://doi.org/10.56714/bjrs.49.2.16)

ABSTRACT

The structural, electric, and optical characteristics of the rock salt (RS) VBi monolayer are studied, together with the phonon transport, using first-principles simulations based on density functional theory (DFT). In addition to its unique electronic properties, the (RS) VBi monolayer also displayed a broad absorption spectrum ranging from visible light to the ultraviolet region. Furthermore, its convergent phonon scattering rate was found to be reduced. These findings highlight the potential of further theoretical and experimental investigations into the electronic structure, optical characteristics of the VBi monolayer. The experimental outcomes have shown that the monolayer of (RS) VBi possesses the characteristic of being a half-metal. In the case of the spin-up configuration, the material exhibited metallic properties as the energy levels intersected the Fermi level. On the other hand, for the spin-down configuration, a gap in energy appeared on both sides of the Fermi level, resulting in the formation of a semiconductor. This is indicated by the presence of a gap between the conduction band and the valence band, with the total energy gap of the compound being determined by the combined magnitude of both gaps. The specific energy gap of the (RS) VBi monolayer was measured to be 0.55 eV, which is half the size of a typical metal's energy gap (0.3 eV). Moreover, the (RS) VBi monolayer exhibited a magnetic moment per unit cell equivalent to $2\mu_B$, demonstrating a strong polarization at the Fermi level due to its half-metal nature.

1. Introduction

Due to its indirect uses in the development of electronic device technology, half-metallic (HM) materials have received the majority of attention recently. Researchers working on spin-electronic devices are fascinated by the half-metallic nature of Heusler alloys. De Groot and his team made the initial discovery of these molecules in two half -heusler compounds (NiMnSb and PtMnSb) in 1983[1-3]. In 2004, Konstantin Novoselov and his team successfully extracted graphene from Craft using a mechanical exfoliation method. This breakthrough discovery opened up new possibilities in the field of

*Corresponding author email : jabbar.khalaf@uobasrah.edu.iq



nanomaterials, as ultra-thin 2D nanomaterials like graphene possess extraordinary physical, magnetic, optical, mechanical, and electronic properties [4,5]. Consequently, these nanomaterials have garnered unprecedented attention and are believed to hold immense potential in optical-electronic devices and a wide range of applications, including transistors, nanoscale devices, catalysts, nano electromechanics, photocatalysis, gas sensors, and optical detectors [6,7]. One specific type of half-metallic material, known as HM, has particularly caught the attention of researchers. These materials display 100% spin polarization at Fermi due to their electronic structure, making them promising candidates for spin-link applications. Over the past 35 years, extensive calculations have been conducted to predict and confirm the existence of various half-metallic ferromagnetic materials. This progress in technology can be attributed to the Moore Act, introduced by Gordon Moore, one of the founders of Intel, in 1965 [8,9]. Moore observed that the number of transistors on a processor chip doubles approximately every two years, while the chip price remains the same [10,11]. This observation prompted Intel to integrate silicon (Si) with integrated circuits, igniting a technological revolution worldwide. Silicon, which has been the go-to microprocessor material for over four decades, has now reached its nanoscale through the utilization of the quantum tunneling effect principle. Over time, researchers have made significant discoveries in the field of materials science, uncovering complete Heusler alloys, and other half-metals (HM) [12]. These unique substances, known as Heusler compounds, have sparked interest among scientists due to their unusual properties. Further investigation into their electronic structure revealed that some of these alloys exhibit characteristics of both metals and semiconductors or insulators [13,14]. This intriguing behavior led to the term "half of the metal ferromagnetism" being coined, as it describes the alloy's ability to exhibit ferromagnetism in only one spin direction. In recent years, significant efforts have been invested in developing reliable methods for producing 2D nanomaterials suitable for various applications [15-17]. Two approaches, namely the top-down and bottom-up methods, have been extensively explored. The top-down method involves removing the van der Waals interaction between stacked layers of bulk-layered crystals to obtain single-layer or low-layer two-dimensional nanomaterials. This technique has seen remarkable advancements and has played a crucial role in the miniaturization of electronic devices such as mobile phones, tablets, and computers. These advancements have greatly improved the functionality, stability, and efficiency of these devices, transforming people's lifestyles [18].

2. Computational methods

The optical, magnetic, electronic, phonon transport, and structural characteristics of a (RS) VBi monolayer are computed in this study using the CASTEP code in combination with density functional theory [19]. These characteristics include: phonon transport, optical, magnetic, and electrical. The exchange-correlation energy has been examined using the PBE approach and generalized gradient approximations (GGA) [20]. The valence electron configurations of V and Bi atoms adopted are $3d^3 4s^2$, $6s^2 6p^3$, respectively. The created system is an (RS) VBi monolayer that has 15 Å inserted in a direction that is perpendicular to the surface of the 2D monolayer in order to eliminate any interactions that may exist between atoms. The constructed system is a (RS) VBi monolayer consisting of $(2 \times 2 \times 1)$ per unit cell. The cutoff energy of 400 eV is used when examining plane waves. Every structure has attained its most relaxed state. The size of the atomic force is less than 0.02 eV/\AA , but the magnitude of the total energy affinity is 10^{-5} eV . To replicate the structural, electrical, magnetic, phonon transport, and optical properties of the (RS) VBi monolayer, a sample is collected from the first Brillouin zone using the coordinates $(15 \times 15 \times 1)$.

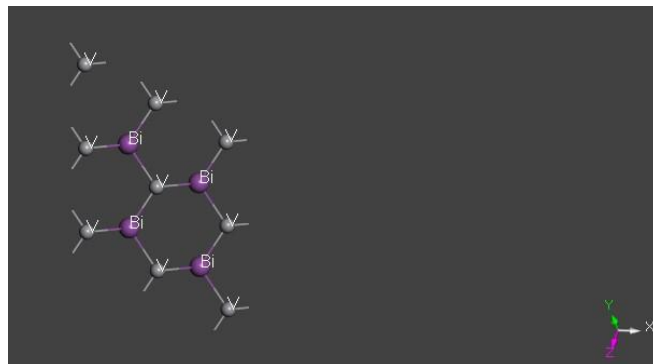


Fig. 1.Crystal structure of (RS) VBi monolayer

3. Results and discussion

3.1 Electronic structures of (RS) VBi monolayer

Structure VBi (Fm3m, No. 225) overall density of states and electronic band structure are depicted in Figure 1. In the equivalence package, the Fermi level at the top of the half-metal gap (HMGap) is 0.3 eV. (V) is more efficient than (Bi) because it has seven electrons that have passed the E_F , two of which are in the s orbital and five of which are in the p orbital [21].

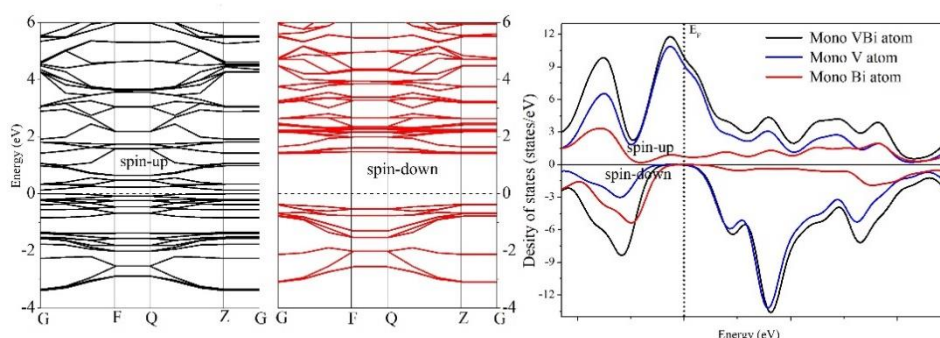


Fig. 2. Band structure (spin \uparrow and spin \downarrow) of VBi (left) and the densities of states of monolayer VBi (right)

3.2 phonon transport

Recent developments in the study of partially metallic materials have highlighted the need for a deeper scientific understanding of heat transfer through materials. To determine the scattering of phonons in the (RS) VBi monolayer, simulation of first-principles calculations based on density functional theory (DFT) is a useful tool. The study of phonons is an essential part of materials physics. In fact, phonons play a crucial role in creating many different physical properties, including electrical conductivity and thermal conductivity. In other words, a phono is the smallest amount of energy that can be transferred from an acoustic source to a physical medium. In this situation, the phonon is like an isotope of electromagnetic waves, that is, the smallest amount of electromagnetic energy that can be transferred from an electromagnetic wave to a physical medium [22]. Figure 2 shows the phonon dispersions of the (RS) VBi monolayer. This figure shows that the monolayer is dynamically stable since the phonon dispersions do not have the imaginary vibrational frequency throughout the Brillouin regime.

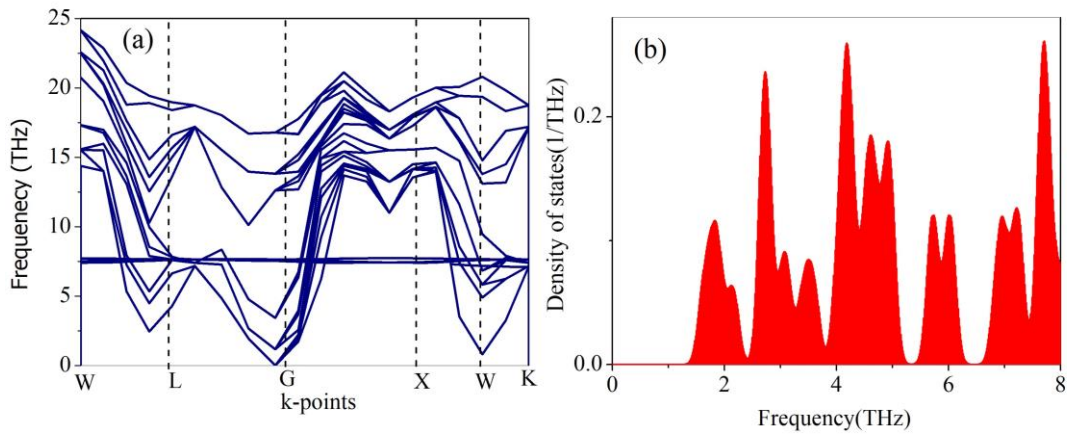


Fig. 2. Curves of phonon dispersion and state density of (RS) VBi monolayer.

3.3 Optical Properties

Two-dimensional materials have improved photovoltaic cells because they have a greater surface area to absorb sunlight, which speeds up the process of light conversion. Optical characteristics of materials are crucial to fundamental research and contemporary applications. We determined the absorption coefficient, reflectivity, loss function, refractive index, propagation constant (K), dielectric function, and conductivity among other optical parameters. It is determined using the relationship shown below.

$$\epsilon(\omega) = \epsilon_1(\omega) + i\epsilon_2(\omega) \tag{1}$$

where the imaginary and real components of the dielectric function are represented by the $\epsilon_1(\omega)$ and $\epsilon_2(\omega)$, respectively. The electromagnetic field's propagative conduct has a connection to reality $\epsilon_1(\omega)$ [23]. The Fermi golden rule is used for adding the occupied–unoccupied transitions to obtain the relationship for the imaginary part $\epsilon_2(\omega)$ [24]. Figure 3 depicts the real and imaginary parts of the dielectric function. The (RS) VBi monolayers has a dielectric function (at zero energy) of is 25×10^5 and 65×10^5 in the real and imaginary components. Additionally, the fact that the real dielectric function is not negative shows that the (RS) VBi monolayer behaves like a semiconductor in this frequency range. While the insulation curve in visible regions grows and lowers with energy, UV radiation drops rapidly with photon energy increase. It is commonly known that materials having gaps less than 1.8 eV perform well in infrared (IR) and visible light. As a result, the RS-VBi monolayer will function as a visual material in the infrared and visible ranges [25].

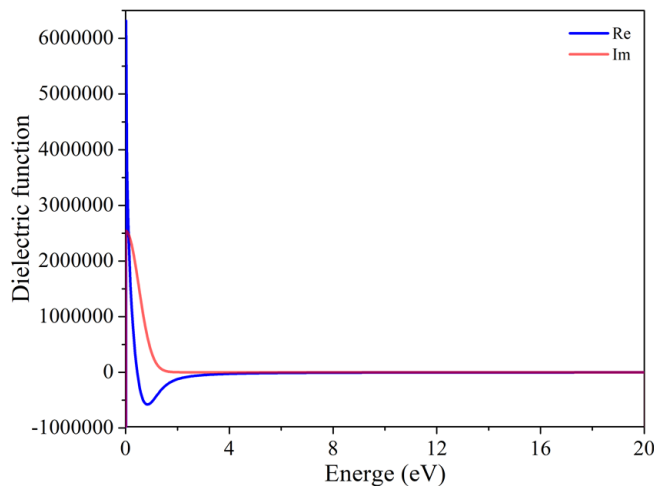


Fig. 3. Imaginary and real components of the dielectric function of the (RS) VBi monolayer

The optical properties were studied in the energy range from 0 to 20 eV. As shown in Figure 4, absorption in the infrared (IR) region starts at values below 0.07 eV of the (RS) VBi monolayer, 8 eV and 1.3 eV. Our results confirmed that there is an infrared (IR) absorption peak in the range between (0.8 eV and 1.3eV). The absorption coefficient shows that its highest peaks are clearly in the ultraviolet range (5 eV). The absorption of visible light begins in the range between (1.5 eV and 3 eV) and is one of the most important research areas on the absorption of light that can be used in the manufacture of solar cells. We also find that a single layer of (RS) VBi monolayer has high ultraviolet radiation absorption energy, which can be used in photoelectronic devices such as UV detectors.

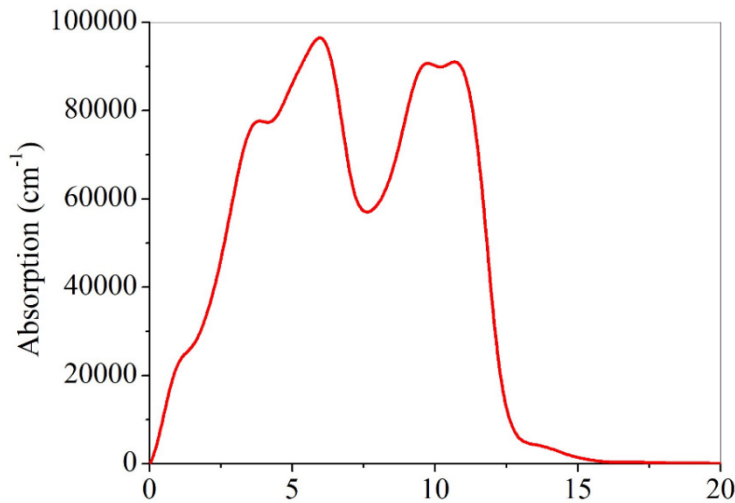


Fig.4. Optical absorption of (RS) VBi monolayer

As a function of photon energy, Figure (5) displays the (RS) VBi monolayer's refractive index and propagation constant. The (RS) VBi monolayer's refractive index and propagation coefficient (at zero energy) are, 7.8 and 1.5, respectively. The propagation constant, on the other hand, has a maximum value of 2.8 at 1.25 eV. The refractive index eventually tends to stabilize at high photon energies, whereas it declines with energy in visible regions and with UV light. The monolayer has a maximum refractive index in the infrared range in general. When the photon's energy reaches 20 eV, the spectra of the refractive index (n) and the propagation constant (K) rapidly decrease and remain constant.

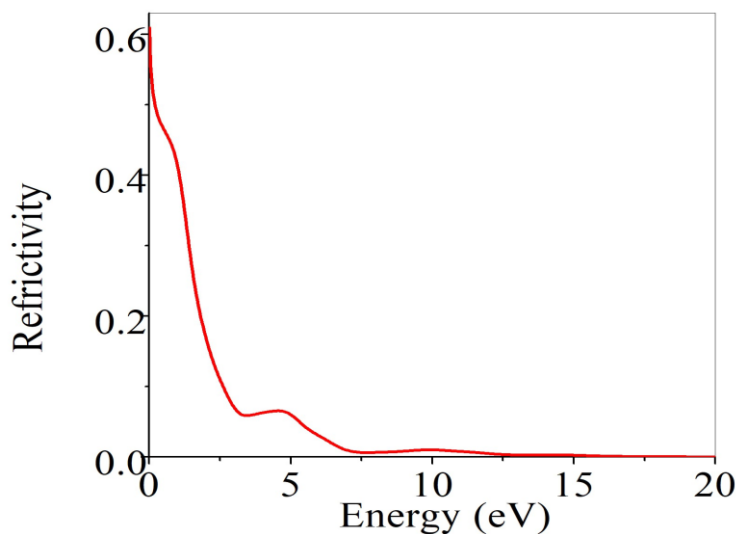


Fig.5. Refractive index and propagation constant of (RS) VBi monolayer

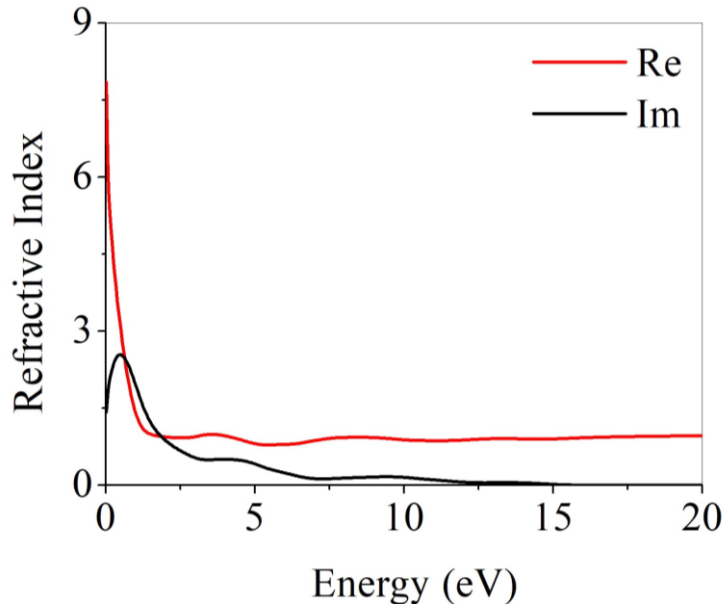


Fig.6. Reflectivity of (RS) VBi monolayer

The predicted optical reflectivity as a function of energy is shown in Figure 6. Optical reflectivity at the zero energy is 0.6 .At 4.5 eV, there is one optically reflective peak for photon energy. The optical reflectivity curve declines with energy in visible regions and rapidly drops as photon energy increases in ultraviolet light. displays the loss function computed as an energy function. We can see that the main steep peak of energy loss for the (RS) VBi monolayer occurs at 1.5 eV for photon energy. This energy indicates the transition from the metal to the insulating state of this (RS) VBi monolayer, which has the potential to be a superb medium-low spectrum radiation absorber. Therefore, the current monolayers can be used in solar cell applications.

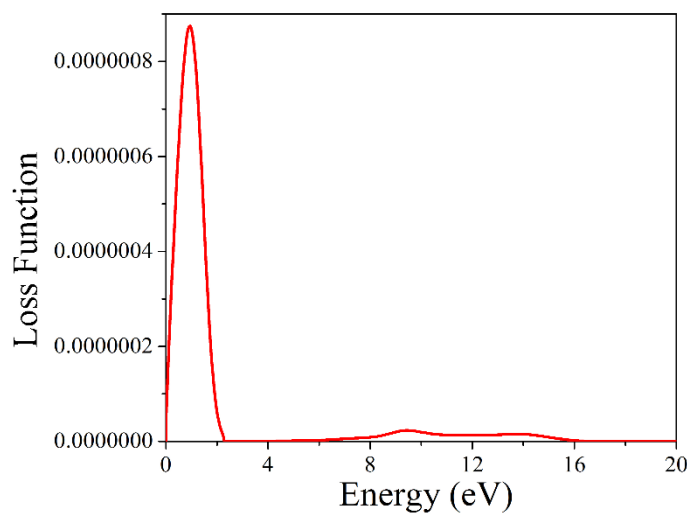


Fig.7. Loss function of (RS) VBi monolayer

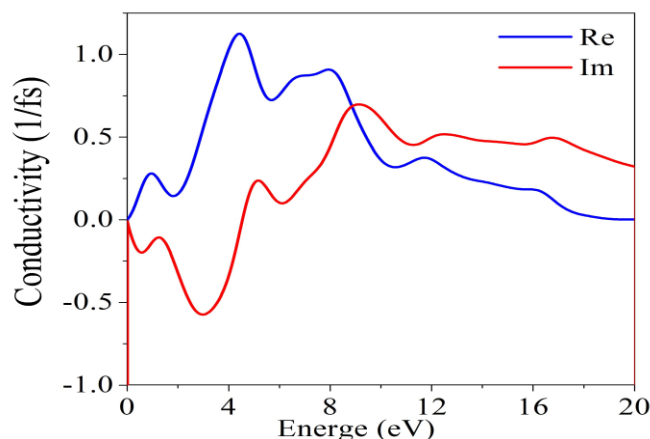


Fig.8.Optical conductivity of (RS) VBi monolayer

Optical conductivity is seen as a function of photon energy in Figure 8. Clearly, the conductivity of the real portion of the (RS) VBi monolayer peaks at 5 eV in the infrared region of 1.3. On the other hand, with photon energy of 10 eV, the maximum values of the imaginary component of conductivity present in the visible ray zone are 0.7.

4. Conclusion

This work considers the electronic structure, optical properties, and phonon transport of the (RS) VBi monolayer through a first-principles investigation. The (RS) VBi monolayer shows half-metallic properties, indicating that the spin-up channel is metallic and the spin-down channel is a semiconductor with an energy gap equal to 0.55 eV. that the amount of magnetic moment per cell unit of the (RS) VBi monolayer is equal to 4 μ_B . The (RS) VBi monolayer is also dynamically stable due to the absence of imaginary phonon vibration frequencies in the entire Brillouin region. The studied optical characteristics determine that the (RS) VBi monolayer is a strong competitor for use in microelectronic and electro-optical applications.

5. Reference

- [1] R. A. de groot, F. M. Mueller, P. G. Van Engen and K. H. J. Buschow, *phys. Rev. Lett* **50**(20), 24 (1983). Doi: <https://doi.org/10.1103/PhysRevLett.50.2024>
- [2] A. Rahman, M.U. Rehman, D. Zhang, M. Zhang, X. Wang, R. Dai, Z. Wang, X. Tao, L. Zhang, Z. Zhang, *Phys. Rev* **550**(50), 246 (2019).Doi: <https://doi.org/10.1039/C9EE01722D>
- [3] K. Elphick, W. Frost, M. Samiepour, T. Kubota, K. Takanashi, S. Hiroaki, S. Mitani, A. Hirohata, *Sci. Technol. Adv. Mater.* **22**(235), 1 (2021).Doi: <https://doi.org/10.1002/est2.448>
- [4] J.Han, R.Cheng, L.Liu, H.Ohno, *Appl.Phys.*, **44**(635), 1 (2023). Doi:<https://doi.org/10.1038/s41563-023-01492-6>
- [5] J.M.K. Al-zyadi, H.I. Asker, K.L. Yao, *Phys. E Low-Dimens. Syst. Nanostruct.* **122**(24), 19 (2020). Doi: <https://doi.org/10.1016/j.elspec.2021.147060>
- [6] R. Y. Umetsu, K. Kobayashi, R. Kainuma, Y. Yamaguchi and K. Ohoyama, A. Sakuma, K. Ishida, J. *Alloys Comp*, **56**(499),1 (2022).Doi: <https://doi.org/10.1016/j.jallcom.2010.02.19>
- [7] G.Y.Gao and K. L. Yao, *J. Appl. Phys.*, **111**, 113703 (2012). Doi: <https://doi.org/10.1063/1.4724339>
- [8] K.S. Novoselov, A.K. Geim, S. V Morozov, D.A. Jiang, Y. Zhang, S. V Dubonos, I.V Grigorieva, and A.A. Firsov **360**(33), 11 (2020).Doi: <https://doi.org/10.1073/pnas.0502848102>
- [9] G.E.Moore, *IEEE Solid-State Circuits Society Newsletter* **11** (3), 37 (2006). Doi:<https://doi.org/10.1109/N-SSC.2006.4785861>

- [10] W.K. Alaarage, A.H. Abo Nasria, and A.H.O. Alkhayatt, *Compu. Theor. Chem.* **1227**, 114223 (2023). Doi: <https://doi.org/10.1016/j.comptc.2023.114223>
- [11] H.R. Jappor, J. Nanoelectron. Optoelectron. **12**(8), 742 (2017). Doi: <https://doi.org/10.1166/jno.2017.2088>
- [12] X. Chen, R. Meng, J. Jiang, Q. Liang, Q. Yang, C. Tan, X. Sun, S. Zhang, T. Ren, *Phys. Chem. Chem. Phys.* **18**, 16302 (2016). Doi: <https://doi.org/10.1039/C6CP02424F>
- [13] H.R. Jappor, and A.S. Jaber, *Sensor Letters* **14**, 989 (2016). Doi: <https://doi.org/10.1166/sl.2016.3722>
- [14] H.R. Jappor, and S.A.M. Khudair, *Sensor Lett.* **15**, 432 (2017). Doi: <https://doi.org/10.1166/sl.2017.3819>
- [15] J.M. Khalaf Al-zyadi, and A.A.-H. Nasser, *Phys. Lett. A*, **458**, 128594 (2023). Doi: <https://doi.org/10.1016/j.physleta.2022.128594>
- [16] K.R. Paton, E. Varrla, C. Backes, R.J. Smith, U. Khan, A. O'Neill, C. Boland, M. Lotya, O.M. Istrate, and P. King, *Nat. Mater.* **13**, 624 (2014). Doi: <https://doi.org/10.1038/nmat3944>
- [17] G. E. Moore, Cramming more components onto integrated circuits, *Electronics*, **38**, 8 (1965).
- [18] M.M. Waldrop, *Nature*. **12**, 144 (2016). Doi: <https://doi.org/10.1038/530144a>
- [19] S.J. Clark, M.D. Segall, C.J. Pickard, P.J. Hasnip, M.I. Probert, K. Refson, and M.C. Payne, *Cryst. Mater.* **55**(15), 11 (20221). Doi: <https://doi.org/10.1524/zkri.220.5.567.65075>
- [20] J.P. Perdew, K. Burke, M. Ernzerhof, *Phys. Rev. Lett.* **456**(12), 441 (1996). Doi: <https://doi.org/10.1103/PhysRevLett.77.3865>
- [21] T. A. Abdel, *J. Supercond. Nov. Magn.* **34**, 1259 (2021). Doi: <https://doi.org/10.1007/s1094802105843-9>
- [22] M. Gajdoš, K. Hummer, G. Kresse, J. Furthmüller, F. Bechstedt, *Phys. Rev. B* **73**, 045112 (2006). Doi: <https://doi.org/10.1103/PhysRevB.73.045112>
- [23] G.Y. Guo, K.C. Chu, D.S. Wang, C.G. Duan, *Phys. Rev. B* **444**(144), 88 (2020). Doi: <https://doi.org/10.1103/PhysRevB.69.205416>
- [24] D.K. Sang, B. Wen, S. Gao, Y. Zeng, F. Meng, Z. Guo, and H. Zhang, *Nanomaterials* **999**(12), 122 (2020). Doi: <https://doi.org/10.3390/nano9081075>

الخصائص الالكترونية و البصرية و الانتقال الفونوني لـ مركب الطبقة الاحادية من VBi بالتركيب الملحي باستخدام مبادئ الحاسبات الاولية

مصطفى محمد جعفر، جبار منصور خلف*

قسم الفيزياء، كلية التربية للعلوم الصرفة، جامعة البصرة، البصرة، العراق.

معلومات البحث	المخلص
الاستلام 15 أيلول 2023	تمت دراسة الخصائص التركيبية والالكترونية والبصرية للطبقة الأحادية VBi للملح الصخري (RS)، جنباً إلى جنب مع نقل الفونون، باستخدام محاكاة المبادئ الأولى القائمة على نظرية الكثافة الوظيفية (DFT). بالإضافة إلى خصائصها الإلكترونية الفريدة، عرضت الطبقة الأحادية VBi (RS) أيضاً طيف امتصاص عريض يتراوح من الضوء المرئي إلى منطقة الأشعة فوق البنفسجية. علاوة على ذلك، تم العثور على أن معدل تشتت الفونون المتقارب الخاص به قد انخفض. تسلط هذه النتائج الضوء على إمكانية إجراء مزيد من التحقيقات النظرية والتجريبية في البنية الإلكترونية والخصائص البصرية للطبقة الأحادية VBi. أظهرت النتائج التجريبية أن الطبقة الأحادية من VBi (RS) تمتلك خاصية نصف معدن. في حالة البرم للأسفل، وأظهرت خواص معدنية حيث تقاطعت مستويات الطاقة مع مستوى فيرمي في حالة البرم للأعلى. يشار إلى ذلك من خلال وجود فجوة بين نطاق التوصيل ونطاق التكافؤ، حيث يتم تحديد فجوة الطاقة الكلية للمركب من خلال المقدار المشترك لكلا الفجوات. تم قياس فجوة الطاقة المحددة للطبقة الأحادية VBi (RS) لتكون 0.55 eV ، و فجوة نصف المعدن النموذجي (0.3 eV). علاوة على ذلك، أظهرت الطبقة الأحادية VBi (RS) عزماً مغناطيسياً لكل خلية وحدة مكافئ $2 \mu\text{B}$ ، مما يدل على استقطاب قوي عند مستوى فيرمي بسبب طبيعتها نصف المعدنية.
القبول 31 تشرين الثاني 2023	
النشر 30 كانون الأول 2023	
الكلمات المفتاحية	
خصائص الطبقة الأحادية، انصاف المعادن، VBi	
Citation: M.M. Jaafar, J. M. Khalaf Al-zyadi, J. Basrah Res. (Sci.) 49(2), 79 (2023). DOI:https://doi.org/10.56714/bjrs.49.2.8	

*Corresponding author email : jabbar.khalaf@uobasrah.edu.iq

